

Light-induced valence-state switching in BaFCl:La and SrFCl:La

M. Matsarski, D. Lovy, H. Bill,* and K. M. Mohnhaupt

Département de Chimie Physique, Sciences 2, 30 quai E. Ansermet, 1211 Genève 4, Switzerland

(Received 5 April 2003; revised manuscript received 16 July 2003; published 26 November 2003)

A tetragonal La^{2+} center (symmetry C_{4v}) was identified in single crystals of BaFCl and SrFCl doped with lanthanum with the aid of electron paramagnetic resonance (EPR)/electron-nuclear double resonance (ENDOR). This center forms a donor-acceptor couple with initially present $\text{F}(\text{F}^-)$ centers. Switching takes place by illumination of appropriate wavelength. The kinetics of the process was monitored by EPR as La^{2+} and the unswitched F center are paramagnetic. The results of our experimental investigation of this kinetics are presented. A foregoing spectroscopic characterization of the La^{2+} center allowed one to identify a $d-d$ (the B_1-E) transition, a charge-transfer band (for BaFCl at $10\,940\text{ cm}^{-1}$ and at $17\,890\text{ cm}^{-1}$, respectively) and to obtain a value of 710 cm^{-1} for the spin-orbit coupling constant in the ground state. In order to narrow the choice of possible acceptor-donor partners a detailed EPR/optical search was further done to identify a number of lattice defects and oxygen centers—in addition to a La-oxygen molecular structure.

DOI: 10.1103/PhysRevB.68.205113

PACS number(s): 72.20.Jv, 76.30.Kg, 71.70.Ej, 71.35.Aa

I. INTRODUCTION

Several PbFCl (matlockite) structure host materials doped with specific rare-earth (RE) ions show promising properties and have for this reason found recent widespread interest, e.g., in the domain of optical spectral hole burning (OSHB) and the one of photostimulated information storage and retrieval. Indeed, several systems (mixed $Me\text{FX}Y$ doped with Sm^{2+} where $Me = \text{Ba}, \text{Sr}$ and $X, Y = \text{Cl}, \text{Br}$) rank still among the best candidates for OSHB applications at room temperature (RT).¹⁻⁵ Other members (BaFBr/BaFCl doped with Eu^{2+}) are at the basis of modern x-ray storage screens, e.g., Refs. 6–8. But important questions regarding microscopic structure(s) and electron transfer processes of the active centers involved are still unanswered and continuing research is needed to gain insight into the underlying processes. The search for “simple” model systems led us to study $Me\text{FCl}$ doped with Lanthanum. We realized that the valence state of this ion is photoswitchable in these hosts, with light from commonly available diode lasers. These systems may contribute clarifying the specific donor acceptor issues. Additionally, they are of interest for spectroscopic reasons because they furnish information on the order and separation of the La^{2+} $5d$ energy levels. As a consequence of the lanthanide contraction⁹ the $4f^n$ configuration is below $4f^{n-1}5d^1$ in the divalent RE ions whereas the ground configuration is $4f^05d^1$ for La^{2+} , which is accessible by ground-state electron paramagnetic resonance (EPR). Two different centers involving lanthanum were identified in several members of the matlockite family with this technique. One of them is photoswitchable, it has tetragonal local symmetry. This paper presents EPR and optical results obtained on BaFCl:La²⁺ and SrFCl:La²⁺. Both hosts have the space group D_{4h}^7 . The crystallographic cation site has point group symmetry C_{4v} . Figure 1 shows the conventional unit cell of this structure. The La^{2+} ions substitute for host cations. A common problem in studying excitation transfer issues of a given impurity is the wealth of possible partners. This is in particular true for matlockite hosts, e.g., Refs. 10, 11, be-

cause an even “ultrapure preparation” condition of a host often results in oxygen being present (in addition to lattice defects) in the as-grown crystals. A detailed EPR study was thus undertaken in parallel on these systems to identify oxygen and defect centers. These results are included in the present paper.

II. EXPERIMENT

All experiments were performed on single crystals. These were grown in our laboratory built Bridgman (typical speed 4 mm/h) and Kyropoulos (typical pulling speed 0.5 mm/h) furnaces, under ultrapure argon with added H_2 or F_2 . The dopant Lanthanum was in the form LaF_3 (99.9% Cerac). During the investigation it became necessary to additionally purify the starting materials, in particular LaF_3 , by their careful fluorination in a laboratory built setup. Several $Me\text{FCl}$ ($Me = \text{Sr}, \text{Ba}$) batches were synthesized directly from $Me\text{F}_2$ and (four times vacuum sublimed) NH_4Cl in a nickel pressure vessel with a graphite liner fitted inside. Transparent and colorless single crystals of typically

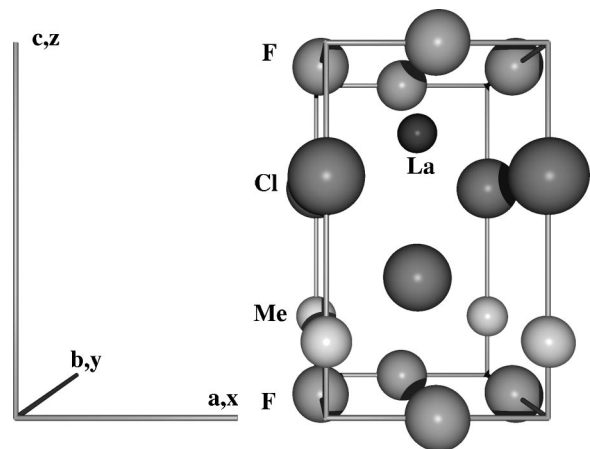


FIG. 1. Conventional unit cell of the PbFCl matlockite structure and axis system used in the paper. Lanthanum is on the central C_4 axis.

0.5–3.0 cm³ resulted. This fact and the absence of any EPR signal in the as-grown crystals proved that lanthanum was incorporated as La³⁺. Appropriately oriented samples were x rayed for 1–6 h (40 kV/20–30 mA, usually at 300 K) resulting in a blue or Bordeaux coloration. Several samples were additively colored by heating them (to 780 °C) in a closed nickel tube under ultrapure argon and in presence of the metal vapor corresponding to the host cation. EPR experiments were performed on a laboratory assembled spectrometer based on a Varian E110 X-band bridge with 100-kHz modulation. A cylindrical TE₀₁₁ mode cavity of our own construction with lateral Suprasil windows (loaded Q typically 7000) was mounted vertically on the top of an Oxford Instruments flow cryostat at the center of the air gap of a Varian 9" magnet. The excitation light setup consisted of an ILC xenon lamp (150–500 W) filtered by an IR absorber followed by a H20 single-grating monochromator (Instruments SA). Its output beam (resolved to ≈ 8 nm at 500 nm) was directed onto the sample in the EPR cavity. The irradiance at the sample crystal (see Table III) was determined. The results are rather estimates as they were determined indirectly: from published tables/graphs of the spectral radiance of the ILC Xe lamp, the response function of the H20 monochromator, and by including optical corrections given by our chosen setup. The light escaping from the crystal was projected onto a Hamamatsu Si-diode detector; Suprasil lenses were used. The electron-nuclear double resonance (ENDOR) setup used the above X-band Varian bridge. A synthesizer (200 kHz–160 MHz) in series with a square-wave modulator (modulation frequency 172 Hz), a wide band preamplifier with current-stabilization feedback, and a power amplifier (300 kHz–120 MHz 250 W and 90–500 MHz 9 W, respectively) supplied the radio frequency (RF) current to the cavity. Details of the cavity and the low-temperature equipment are described in Ref. 12. The spectrometer is fully computer controlled (see Ref. 12 which describes the basic setup). The analysis of the EPR and ENDOR spectra was performed as described, for instance, in Ref. 13. Optical-absorption measurements were realized on a Cary 2300 instrument or on a modified Unicam SP800 (200–800 nm) instrument.

III. RESULTS

A. Spectroscopic identification of the dominant centers

The x-irradiated samples presented EPR spectra due to lanthanum, which were function of the crystal-growth conditions. In addition all of them showed EPR signals due to lattice defects and most of the samples exhibited EPR signals due to oxygen.

1. Tetragonal lanthanum center

The samples originating from crystals which had been grown by using fluorinated LaF₃ (typically 0.1–0.2 %) and either BaCl₂ of low oxygen content or NH₄Cl (see above) presented after x irradiation the EPR spectrum of a tetragonal La²⁺ center. Figure 2 shows the spectrum of BaFCl:La²⁺ obtained with $B\|C_4$. The electron spin of La²⁺ ion is $S = 1/2$. The corresponding $M_s = 1/2 \leftrightarrow M_s = -1/2$ EPR transi-

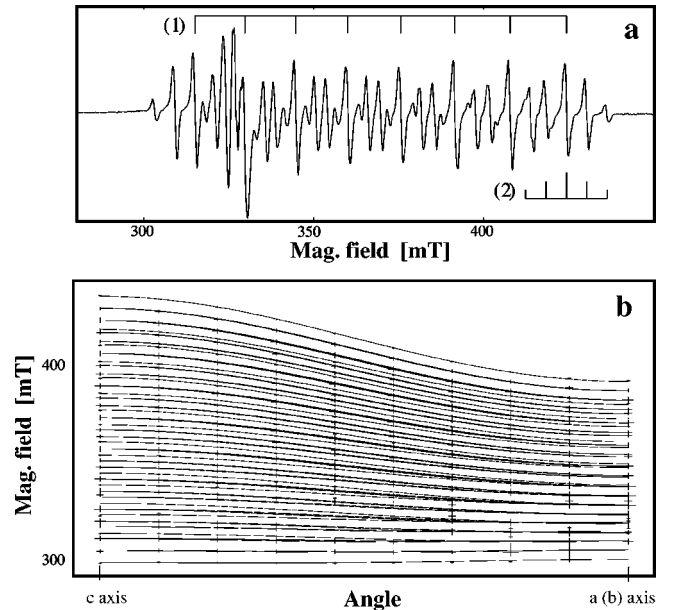


FIG. 2. (a) EPR spectrum of tetragonal La²⁺ in BaFCl: $B\|C_4$. $\nu = 9086.1$ MHz, $T = 5$ K. (b) Angular dependence of the EPR spectrum: $B\|(100)$. Crosses, experimental points and continuous lines, best fit with the parameters of Table I. T and ν have same values as (a).

tion splits into eight lines due to the hyperfine (hf) interaction with the lanthanum nuclear spin (99.8% with $I = 7/2$) [see Fig. 2(a), sticks labeled (1)]. Each hf transition is further split into a number of lines due to the superhyperfine (shf) interaction with the four structurally equivalent direct F⁻ neighbor nuclei. When these are equivalent with respect to B 5 shf lines result having relative intensities 1:4:6:4:1. This situation applies in particular when $B\|C_4$ as shown in Fig. 2(a). The sticks labeled (2) in this figure point to one of these shf structure quintets. The spectrum concurs fully with the proposed model of the center. The angular dependence of the spectrum in the (100) planes [Fig. 2(b)] and the (001) plane (not shown) gave further evidence for the model. Similar results were obtained for SrFCl:La²⁺. The EPR spectra of both systems, SrFCl:La²⁺ and BaFCl:La²⁺, were parametrized with the aid of the following spin Hamiltonian.

$$H = \beta_B S \cdot g \cdot B + S \cdot A^{La} \cdot I^{La} + \sum_{\mu} (S \cdot A^{\mu} \cdot I^{\mu} - g_{N,\mu} \cdot \beta_N \cdot B \cdot I_{\mu}). \quad (1)$$

The symbols have their usual meaning. The axes of the tetragonal g and A^{La} tensors are parallel to the ones shown in Fig. 1. The index μ enumerates the observed neighboring fluorine nuclei. The shf structure tensors A^{μ} have monoclinic symmetry. An initial parametrization was undertaken by assuming that they contain an antisymmetric part. The resulting values of this part were below the errors of the experiment. For this reason A^{μ} were assumed symmetric. The orientation of their respective axis systems is obtained by applying the sequence of rotations with the Euler angles α then β then γ to the axes x, y, z of Fig. 1. The obtained

TABLE I. EPR spin Hamiltonian parameters of tetragonal La^{2+} in SrFCl (at 78 K and 5 K) and BaFCl (at 5 K).

Host	Defect	g_{\parallel}	g_{\perp}	$-A_{\parallel}^{\text{La}}$	$-A_{\perp}^{\text{La}}$	$ A_{xx}^{\text{F}} $	$ A_{yy}^{\text{F}} $	$ A_{zz}^{\text{F}} $	β [$^{\circ}$] ^a	T [K]
SrFCl	La^{2+}	1.7931(2)	1.8963(3)	397.14(4)	276.6(5)	125(8)	123(8)	156(7)	26(10)	78
SrFCl	La^{2+}	1.7900(3)	1.8971(4)	402.3(6)	274.6(7)	123(5)	130(4)	157(8)	13(8)	5
BaFCl	La^{2+}	1.7533(1)	1.8891(2)	383.1(3)	262.4(5)	121(4)	132.4(4)	148(8)	15(8)	5

^aEuler angles $\alpha, \beta, \gamma, \alpha=0^{\circ}, 90^{\circ}, 180^{\circ}, 270^{\circ}, \gamma=0^{\circ}$.

spin-Hamiltonian parameters are given in Table I. In both cases no resolved shf structure due to Cl^{-} ions was observed by EPR. At 4.2 K it was possible to saturate both systems with a microwave power of 1–4 mW and ENDOR experiments were performed to improve the precision of the fluorine shf constants. ENDOR lines due to Cl^{-} were observed but not investigated in detail. The respective temperature dependences of the relaxation times are rather different for the two hosts. The lanthanum EPR signal disappeared at ≈ 40 K in BaFCl but was observed up to ca. 130 K in SrFCl.

Optical-absorption bands associated with this ion were identified with the aid of correlated optical and EPR experiments. They were at $17\,890\text{ cm}^{-1}$ (FWHH: 3030 cm^{-1}) and at $10\,940\text{ cm}^{-1}$ (integrated intensity = $0.09 \times$ intensity of the former one) for BaFCl: La^{2+} . The corresponding bands were at $16\,780\text{ cm}^{-1}$ (FWHH: 1700 cm^{-1}) and at $\approx 11\,600\text{ cm}^{-1}$ (integrated intensity = $0.01 \times$ intensity of the former band) for SrFCl: La^{2+} . The bands were of nearly Gaussian shape and the surface under the curve of the bands in the visible part of the spectrum was only weakly temperature dependent. These transitions are nearly allowed. This is not contradicted by a value of $0.15(\pm 0.04)$ of their oscillator strength deduced with the Dexter-Smakula equation. The concentration of the tetragonal lanthanum centers was thereby determined by comparing the integrated EPR signal intensity with the equivalent quantity of a known quantity of CuSO_4 along known procedures. The bands in the visible part were unpolarized.

2. Monoclinic lanthanum-oxygen molecule ion

Samples originating from crystals that had been grown by using as-bought LaF_3 and/or vacuum-dried BaCl_2 presented after x-irradiation an EPR spectrum of monoclinic symmetry with respect to $\{110\}$. The signals were observed already at room temperature. The angular dependence of the spectrum was studied in detail and was parametrized with the aid of the first two terms of Eq. (1). The resulting spin-Hamiltonian parameters are given in Table II. The z axis of the monoclinic g tensor is rotated in (110) by 65° from C_4 for SrFCl and by 47° for BaFCl. Both systems present an isotropic lanthanum hyperfine tensor A^{La} . This center clearly includes one lanthanum atom. It also includes oxygen for the following reasons.

(1) Its spin-Hamiltonian parameters and optical-absorption spectrum (see below) are very similar to the ones of the Yttrium-Oxygen center in the alkaline-earth fluorides.¹⁴

(2) The MeFCl crystals ($\text{Me}=\text{Sr}, \text{Ba}$) grown under oxygen-free conditions (see Sec. II) did not show this center.

But when during crystal growth a few 100–1000 ppm of MeO was added to the melt or when oxygen-free crystals were subsequently hydrolized (see, e.g., Ref. 15) the monoclinic lanthanum center was always observed after subsequent x irradiation of these samples. An optical transition at $22\,370\text{ cm}^{-1}$ (SrFCl) and at $20\,400\text{ cm}^{-1}$ (BaFCl), respectively, was found to be due to this center. Its integrated intensity was nearly independent of temperature for $T \leq 300$ K. The whole of the results made evident the close similarity between this center and the well known YO and YO_2 molecular structures observed in the alkaline-earth fluoride hosts.^{14,15}

For all these reasons part of the samples presented simultaneously the tetragonal La^{2+} center and this molecular La-O structure. Nevertheless, the two centers were easily distinguished in EPR experiments due to the very different temperature dependences of the respective relaxation times.

3. X-radiation damage and oxygen centers in MeFCl ($\text{Me}=\text{Sr}, \text{Ba}$)

All our x-irradiated and/or additively colored samples of SrFCl and BaFCl presented the corresponding $\text{F}(\text{F}^{-})$ center (see Table II). The samples which had been additively colored additionally presented the EPR spectrum of the corresponding $\text{F}(\text{Cl}^{-})$ center. The spin-Hamiltonian constants of these F centers were determined (see Table II) and the optical-absorption spectra recorded. The obtained results fully agree with the ones determined by Yuste *et al.*¹¹ in pure MeFCl .

Several EPR spectra due to oxygen centers were observed in both hosts. The angular variation of the dominant spectra was studied in detail and analyzed. The resulting spin-Hamiltonian parameters are given in Table II. Generally speaking, the basic oxygen centers $\text{O}^{-}(\text{F}^{-})$, $\text{O}^{-}(\text{Cl}^{-})$, and $\text{O}_2^{-}(\text{Cl}^{-})$ in BaFCl are well understood.^{7,10} Our results agree with the published ones as regards these systems. The situation is different for SrFCl where very few published results exist (see, however, Ref. 16). This will be discussed in Sec. IV. Note that the published results about the oxygen centers in BaFCl had been obtained from crystals only doped with oxygen. The good agreement between these and our corresponding results shows that our oxygen centers in BaFCl are not located in the immediate neighborhood of lanthanum (see also Ref. 17), with the exception, of course, of the LaO molecular structure.

B. Light-induced electron transfer processes

A large part of the investigation focused onto the processes in the BaFCl host. These will be presented in the

TABLE II. Principal values of the g tensors of several centers and of the La-oxygen complex in SrFCl and BaFCl.

Host	Defect	g_{xx}	g_{yy}	g_{zz}	α [°]	β [°]	γ [°]	T [K]	Remarks ^a	Ref.
SrFCl	F(Cl ⁻)	1.9927	1.9927	1.9945	0	0	0	78	shfs resolved only along c	11
	F(F ⁻)	1.993	1.993	1.997	0	0	0	77	shfs resolved only along c	11
	O ⁻ (Cl ⁻) ^I	2.0602	2.0602	2.0024	0	0	0	77	shfs 4 F $A_{xx}=10.9$ MHz $A_{yy}<2.0$ MHz $A_{zz}=40.5$ MHz $\alpha=0^\circ, 90^\circ, 180^\circ, 270^\circ$ $\beta=38(4)^\circ, \gamma=0^\circ$	this paper, see text
	O ⁻ (Cl ⁻) ^{II}	2.1746	2.1746	1.9925	0	0	0	77	shfs 4 F $A_{xx}=54.5$ MHz $A_{yy}=45.8$ MHz $A_{zz}=12.4$ MHz $\alpha=0^\circ, 90^\circ, 180^\circ, 270^\circ$ $\beta=44(6)^\circ, \gamma=0^\circ$	this paper, see text
	O ₂ ⁻ (Cl ⁻)	2.1088	2.0063	2.0005	0	0	0	77	shfs 2 F $A_{xx}=11$ MHz $A_{yy}<6$ MHz $A_{zz}=43$ MHz $\alpha=0^\circ, 180^\circ$ $\beta=38(5)^\circ, \gamma=0^\circ$	this paper, see text
	O ₂ ⁻	2.1365 2.097	1.9536 1.96	1.9613 2.003	0 0	29(5) 0	0 0	4.4 32	No resolved shfs Motional averaging in (100) Spectrum disappears for $T \geq 36$ K	this paper, see text
O ₂ ⁻ -V _F (?)	LaO	2.0038	2.0038	2.0819	0	33(5)	0	77	No resolved shfs	this paper
	LaO	2.0401	2.0299	1.9956	45	65(4)	0	77	$A_{iso}^{La}=43.5$ MHz ($I^{La}=7/2$)	this paper, see text
BaFCl	F(Cl ⁻)	1.9798	1.9798	1.9690	0	0	0	77	shfs 4 (Ba ¹³⁵ , Ba ¹³⁷)	11
	F(F ⁻)	1.9695	1.9695	1.9836	0	0	0	77	shfs 4 (Ba ¹³⁵ , Ba ¹³⁷)	11
	O ⁻ (Cl ⁻)	2.2476	2.2476	1.9770	0	0	0	77	shfs 4 F	10
	O ⁻ (F ⁻)	2.0881	2.0881	2.0015	0	0	0	77	shfs 4 (Cl ³⁵ , Cl ³⁷)	10
	O ₂ ⁻ (Cl ⁻)	2.2375	1.9941	1.9868	0	0	0	15	shfs 2 F	10
	O-V _F (?)	1.9952	1.9952	2.0576	0	36(5)	0	77		this paper
	O-V _{Cl} (?)	2.0049	2.0049	2.1207	45	45(4)	0	77		this paper
	LaO	2.0591	2.0106	2.0022	45	47(4)	0	77	$A_{iso}^{La}=43$ MHz	this paper, see text

^ashfs constants are absolute values.

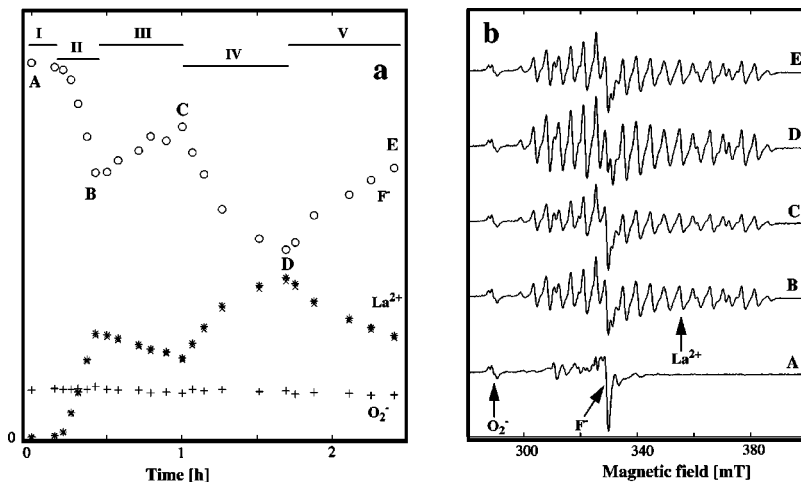


FIG. 3. (a) Intensity of the EPR lines labeled by arrows in (b) as a function of time under different lighting conditions (I, no light; II, IV, 400 nm; and III, V, 700 nm). Host: BaFCl. (b) The spectra observed at times denoted by A, . . . , E in (a): $B_{\parallel}[110]$, $\nu=9092.5$ MHz, and $T=20$ K. \circ , F(F⁻); \bullet , La²⁺; + and O₂⁻(Cl⁻).

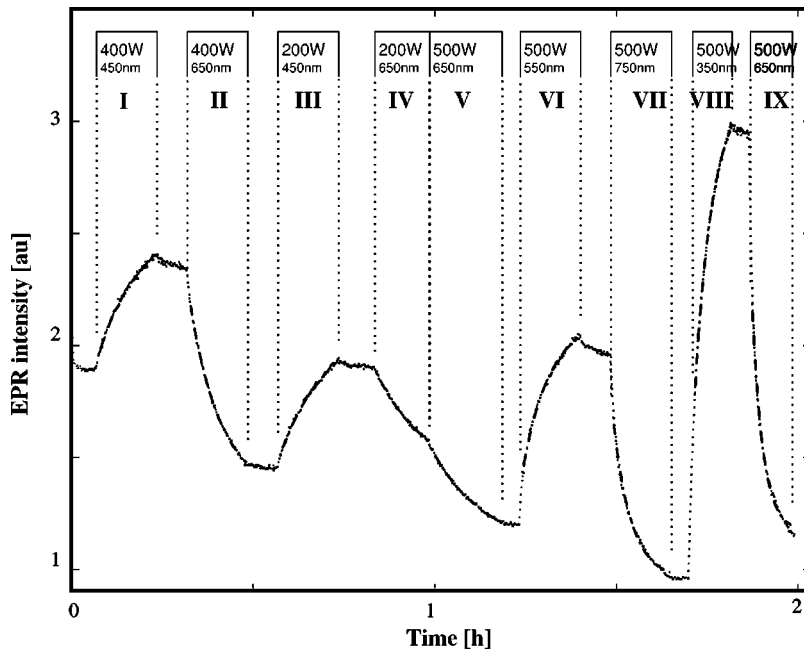


FIG. 4. Evolution of the $\text{La}_{\text{tet}}^{2+}$ EPR signal as a function of the wavelength and nominal power of the impinging light. Host: BaFCl, $B = 355.30$ mT. $B \parallel a(b)$ axis, $T = 5$ K, and $\nu = 9093.0$ MHz. Dots, measured points and dashed line, best fit with the parameters reported in Table III.

following. As the F centers are intrinsically unstable at RT (Refs. 11,18) experiments were performed at typically 5 K.

The effect of the light was monitored with the aid of EPR. Briefly irradiated samples of BaFCl:La were chosen which did not present the La^{2+} spectrum but showed $\text{O}_2^-(\text{Cl}^-)$, $\text{O}^-(\text{F})$ and $\text{F}(\text{F}^-)$ with a good signal-to-noise ratio (S/N) [spectrum A in Fig. 3(b)]. Then, different lighting conditions were applied and the EPR spectrum was repetitively recorded. The spectra of several runs are shown in Fig. 3(b). They corresponded to times labeled A(start), B, . . . , E(end) in Fig. 3(a). The intensities of the three EPR lines marked by arrows in Fig. 3(b) are plotted in Fig. 3(a). The treatments were the following

(I) No light applied: no changes were seen.

(II) Light of wavelength 400 nm was switched on. The global reaction $\text{F}(\text{F}^-) + \text{La}^{3+} + h\nu \rightarrow \text{F}^+(\text{F}^-) + \text{La}^{2+}$ took place.

(III) The wavelength of the light was switched to 700 nm. A reverse process took place (see Sec. IV).

(IV,V) Repetition of the cycle (II, III).

The concentration of the O_2^- centers remained unaffected [see Figs. 3(a) and 3(b)]. The $\text{F}(\text{F}^-)$ center and La^{2+} showed donor-acceptor behavior. Their respective states were switchable by light of appropriate wavelengths. Similar experiments were performed on SrFCl: La^{2+} at 78 K sample temperature. The electron transfer between the F centers and the lanthanum ions was observed also in this case (but see below). In addition, some samples presenting a useable $\text{O}^-(\text{Cl}^-)$ center concentration permitted a light-induced back-and-forth electron transfer between this one and the lanthanum ions. Only few experiments were performed at RT. The evolution of the tetragonal La^{2+} center concentration was thereby monitored with the aid of the optical absorption band in the visible. The fact that the F centers are metastable at RT had to be taken into account.

The time dependence of the La^{2+} concentration was further recorded at several different wavelengths of the exciting

light. The magnetic field of the EPR spectrometer was tuned to the maximum of the transition marked by the arrow in Fig. 3(b) of the La^{2+} spectrum (B). The exciting light was set to different wavelengths and powers and the intensity of the transition was continuously monitored. The results are presented as points in Fig. 4. The superimposed dashed line represents the best fit obtained from the rate equation given in the caption of Table III, with the aid of a MATLAB script and by using the parameters given in this table.

Globally, there was close but not exact reversibility. After several back-and-forth transfers a broad and weak optical-absorption band (peaking at 14065 cm^{-1} in BaFCl) began to appear. No EPR signal could be associated to it but the wavelength region corresponds to absorption bands of (non-paramagnetic) F center aggregates.^{19–21,18} Subsequent heating of the samples (to 200°C for about 10–15 min) made the coloration disappear. The electron transfer processes between the $\text{La}_{\text{tet}}^{2+}$ ion and $\text{F}(\text{F}^-)$ in SrFCl:La were observed only in samples of low oxygen content. The presence of small con-

TABLE III. Parameters of the fit of the curves Fig. 4. The fit function was $S = C + A \exp[-\kappa_0 t]$ (see text).

No.	λ (nm)	P [irrad. (mW/cm ²)/ nom. power xe-lamp (W)]		κ_0 (min ⁻¹)	A (a.u.)	C (a.u.)
I	450	0.35/400		0.149	-0.61	2.54
II	650	0.17/400		0.197	0.93	1.34
III	450	0.17/200		0.137	-0.61	2.10
IV	650	0.087/200		0.114	0.50	1.39
V	650	0.22/500		0.114	0.46	1.09
VI	550	0.37/500		0.223	-0.74	2.12
VII	750	0.14/500		0.340	0.80	0.96
VIII	350	0.23/500		0.337	-1.51	3.14
IX	650	0.22/500		0.575	1.21	1.17

centrations of oxygen, more specifically of the O^- centers, turned out to be more critical than in BaFCl as the electron transfer processes involved in addition the oxygen centers. Rate constants measured in samples with low oxygen content were typically 25–40 % smaller than the corresponding ones observed in BaFCl:La²⁺. But the non-negligible dependence on oxygen centers would have needed one to perform a much more detailed study of these systems, which has not been done.

IV. DISCUSSION

To our knowledge there are few publications on optical and EPR properties of La²⁺ impurities^{22–25} to compare with. In addition the cited papers all deal with a Jahn-Teller (JT) ground state. The ground state of the present system is orbitally nondegenerate and transforms as B_1 under the C_{4v} point group. It is mainly $5d_{x^2-y^2}$. The orbital reduction factor^{26,27} deduced from the fluorine shf structure is $k \approx 0.86$ for La_{site}La²⁺ in BaFCl and $k \approx 0.83$ in SrFCl. We assigned the optical-absorption band at $10\,940\text{ cm}^{-1}$ to the (only symmetry-allowed) $B_1 \rightarrow E$ transition within the d manifold of La_{site}La²⁺. This allowed one to obtain an estimate of the spin-orbit coupling constant by using the relation $g_{\perp} - 2.0023 = (2k\lambda/\Delta_{BE})$.^{26,27} The evaluation gave $\lambda = 710 (\pm 20)\text{ cm}^{-1}$. This approach needed one to consider, however, that the terminal E state is degenerate and, therefore, is JT active. The coupling between this state and the zone-center b_1 phonon (where b_1 is the optical Raman-active Γ -point phonon at 216 cm^{-1} e.g., Ref. 28) is probably strongest, thus a model ($E \otimes b_1$) applies. With the aid of the model of Bacci²⁹ which includes this situation we estimated a JT energy of the E manifold of 155 cm^{-1} which justifies the approximation used to obtain λ . These results allowed one to further predict the position of the $B_1 \rightarrow E$ transition in SrFCl. The evaluation gave an electronic transition energy of $11\,400\text{ cm}^{-1}$, which is in good agreement with our preliminary experimental result. We identify the absorption bands at $17\,890\text{ cm}^{-1}$ for BaFCl and at $16\,780\text{ cm}^{-1}$ for SrFCl as charge-transfer transitions, in agreement with their respective oscillator strength.}}

Several of the oxygen centers listed in Table II need to be examined, in particular regarding the host SrFCl. There, no $O^-(F^-)$ has been identified reproducibly. The $O^-(Cl^-)^I$ ion shows a shfs which is the signature of a Cl^- site. It was observed with a very good S/N ratio in the pure (only oxygen-containing) SrFCl host and was absent or generally rather weak in the La-doped ones. On the contrary, the $O^-(Cl^-)^{II}$ ion was only observed in the RE-doped samples. Its shfs indicates that this O^- ion has tetragonal site symmetry and is located on or near a Cl^- position—probably associated with a nearby vacancy on the C_4 axis. This tentative model has to be tested and probably completed as we observed this center only in the RE-doped SrFCl crystals. The $O_2^-(Cl^-)$ molecule ion is very similar to the one identified in BaFCl which is very well documented (see Refs. 6,7,10, and references therein). The O_2^- center showing motional effects

above 18 K in its EPR spectrum is remarkable. Indeed, the orientation of its magnetic orbital is along $[100]$, in a geometry where the molecular and the third orthogonal axes are located in a corresponding (100) crystallographic plane. The motional effects affect these latter two axes. This center is probably situated at an interstitial position located in (100), in line with a stable interstitial site predicted from numerical simulations by Islam and Baetzold.³⁰ Two in-plane host cations are disposed symmetrically with respect to the C_2 axis passing through the site. At its low-temperature monoclinic position the oxygen molecule ion is off the site and interacts dominantly with one of the cations. At higher temperatures it switches between the two symmetrically and energetically equivalent positions. Thereby it restores dynamically the local symmetry C_{2v} as observed by EPR. The oxygen centers associated with a question mark have been identified experimentally with a good S/N, but the given models are only tentative.

The time evolution of the La²⁺ density (Table III and Fig. 4) presents a dominant transfer mechanism of the type $D \rightleftharpoons I$. The constant κ_o of this table is a function of the forward k_1 (D to I) and the backward k_2 rate constant, respectively, and of the intensity and frequency of the excitation light. It further includes the transition probabilities of the intervening excitation processes.

A remarkable fact is that the La²⁺ concentration decreased under irradiation with light of $\lambda = 13\,300\text{ cm}^{-1}$ (750 nm). At this energy no optical transition due to the tetragonal La²⁺ impurity could be observed. Nevertheless, the La²⁺ concentration decreased with a specific (normalized with respect to the irradiance) rate comparable to the one obtained with light at $15\,385\text{ cm}^{-1}$. The question is, therefore, whether the conversion from La²⁺ to La³⁺ is at the end due to an electron transferred from the ion to the lattice or due to a hole trapped from the lattice. The second hypothesis seems more likely in view of the obtained results. Our data demonstrate the presence of F center aggregates^{19–21,18} which have a ground-state energy located in the band gap but with energy depending on the number of vacancies and electrons involved. Excitation into the absorption bands of some of these may result in a rearrangement of the electron distribution such that a hole is created. This cannot be a simple V_K center, as these remain localized at 20 K. Instead, probably an electron-hole pair is created which diffuses into the lattice where it encounters a La²⁺. The hole is captured and the electron is attracted by an ionized F center. This mechanism agrees with the fact that no V_K centers were observed and shows the importance of the cluster F centers for the return transfer mechanism. It would be important to be able to associate photoconductivity experiments with the presently reported ones to be able to assess the position of the different F center species in the energy gap of the crystal.

ACKNOWLEDGMENTS

This research was supported by the Swiss National Science Foundation (Grant No. 21-50828.97) and by the Swiss Optics Priority Program No. 2.

*Electronic address: hans.bill@chiphy.unige.ch

- ¹W.E. Moerner, *Persistent Spectral Hole Burning: Science and Applications*, Topics in Current Physics, Vol. 44 (Springer, Berlin, 1988).
- ²R.M. Macfarlane, *J. Lumin.* **100**, 1 (2002).
- ³R. Jaaniso and H. Bill, *Europhys. Lett.* **16**, 569 (1991).
- ⁴J. Zhang, S. Huang, and J. Yu, *Opt. Lett.* **17**, 1146 (1992).
- ⁵K. Holliday, C. Wei, M. Croci, and U.P. Wild, *J. Lumin.* **53**, 227 (1992).
- ⁶L.H. Brixner, *Mater. Chem. Phys.* **16**, 213 (1987).
- ⁷T. Hangleitner, T.K. Koschnick, J.-M. Spaeth, R.H.D. Nuttall, and R.S. Eachus, *J. Phys.: Condens. Matter* **2**, 6837 (1990).
- ⁸G. Blasse, *J. Alloys Compd.* **192**, 17 (1993).
- ⁹M. Goepfert-Mayer, *Phys. Rev.* **60**, 184 (1941).
- ¹⁰R.S. Eachus, R.H.D. Nuttall, M.T. Olm, W.G. McDugle, F.K. Koschnick, T. Hangleitner, and J.-M. Spaeth, *Phys. Rev. B* **52**, 3941 (1995).
- ¹¹M. Yuste, L. Taurel, M. Rahmani, and D. Lemoyne, *J. Phys. Chem. Solids* **37**, 961 (1976).
- ¹²C. Balestra, H. Bill, and J.-L. Clignez, *J. Phys. E* **12**, 824 (1979).
- ¹³J. Rey, H. Bill, D. Lovy, and H. Hagemann, *J. Alloys Compd.* **274**, 164 (1998).
- ¹⁴H. Bill, *Helv. Phys. Acta* **42**, 771 (1969).
- ¹⁵F. Deyhimi and H. Bill, *Chem. Phys. Lett.* **78**, 603 (1981).
- ¹⁶R. Jaaniso, H. Hagemann, F. Kubel, and H. Bill, *Chimia* **46**, 133 (1992).
- ¹⁷C.H. Anderson and E.S. Sabisky, *Phys. Rev. B* **3**, 527 (1971).
- ¹⁸T. Kurobori, M. Kawabe, M. Liu, and Y. Hirose, *Jpn. J. Appl. Phys., Part 2* **39**, L629 (2000).
- ¹⁹W. Chen, Q. Song, and M. Su, *J. Appl. Phys., Part 1* **81**, 3170 (1997).
- ²⁰C. Wei, W. Zhanguo, L. Lanying, and S. Mianzeng, *J. Phys. Chem. Solids* **59**, 49 (1998).
- ²¹T. Kurobori, S. Kozake, Y. Hirose, K. Somaiah, K. Inabe, M. Ohimi, and M. Haruna, *Jpn. J. Appl. Phys., Part 2* **37**, L812 (1998).
- ²²W. Hayes and J.W. Twidell, *Proc. R. Soc. London, Ser. A* **82**, 330 (1963).
- ²³J.R. Herrington, T.L. Estle, and L.A. Boatner, *Phys. Rev. B* **3**, 2933 (1971).
- ²⁴J.R. Herrington, T.L. Estle, and L.A. Boatner, *Phys. Rev. B* **7**, 3003 (1973).
- ²⁵H. Bill and O. Pilla, *J. Phys. C* **17**, 3263 (1984).
- ²⁶A. Abragam and B. Bleaney, *Electron Paramagnetic Resonance of Transition Metal Ions* (Clarendon Press, Oxford, 1970).
- ²⁷S. Sugano, Y. Tanabe, and H. Kamimura, *Multiplets of Transition Metal Ions in Crystals* (Academic Press, New York, 1970).
- ²⁸D. Nicollin and H. Bill, *J. Phys. C* **11**, 4803 (1978).
- ²⁹M. Bacci, *Phys. Rev. B* **17**, 4495 (1978).
- ³⁰M.S. Islam and R. Baetzold, *J. Phys. Chem. Solids* **53**, 1105 (1992).